BIOCHEMISTRY
including biophysical chemistry & molecular biology

Accelerated Publication

pubs.acs.org/biochemistry

A Radical Transfer Pathway in Spore Photoproduct Lyase

Linlin Yang,[†] Renae S. Nelson,[†] Alhosna Benjdia,*[,∥] Gengjie Lin,[†] Joshua Telser,[‡] Stefan Stoll,*[,§] Ilme Schlichting,[∥] and Lei Li*[,†]

[†]Department of Chemistry and Chemical Biology, Indiana University-Purdue University Indianapolis, Indianapolis, Indiana 46202, United States

[‡]Department of Biological, Chemical, and Physical Sciences, Roosevelt University, Chicago, Illinois 60605, United States

[§]Department of Chemistry, University of Washington, Seattle, Washington 98195, United States

[∥]Department of Biomolecular Mechanisms, Max-Planck Institute for Medical Research, Jahnstrasse 29, 69120 Heidelberg, Germany

Supporting Information

ABSTRACT: Spore photoproduct lyase (SPL) repairs a covalent UV-induced thymine dimer, spore photoproduct (SP), in germinating endospores and is responsible for the strong UV resistance of endospores. SPL is a radical *S*-adenosyl-L-methionine (SAM) enzyme, which uses a $[4Fe\text{-}4S]^{+}$ cluster to reduce SAM, generating a catalytic 5′-deoxyadenosyl radical (5′-dA$^{\bullet}$). This in turn abstracts a H atom from SP, generating an SP radical that undergoes β scission to form a repaired 5′-thymine and a 3′-thymine allylic radical. Recent biochemical and structural data suggest that a conserved cysteine donates a H atom to the thymine radical, resulting in a putative thiyl radical. Here we present structural and biochemical data that suggest that two conserved tyrosines are also critical in enzyme catalysis. One [$Y99_{(Bs)}$ in *Bacillus subtilis* SPL] is downstream of the cysteine, suggesting that SPL uses a novel hydrogen atom transfer (HAT) pathway with a pair of cysteine and tyrosine residues to regenerate SAM. The other tyrosine [$Y97_{(Bs)}$] has a structural role to facilitate SAM binding; it may also contribute to the SAM regeneration process by interacting with the putative $^{\bullet}Y99_{(Bs)}$ and/or 5′-dA$^{\bullet}$ intermediates to lower the energy barrier for the second H abstraction step. Our results indicate that SPL is the first member of the radical SAM superfamily (comprising more than 44000 members) to bear a catalytically operating HAT chain.

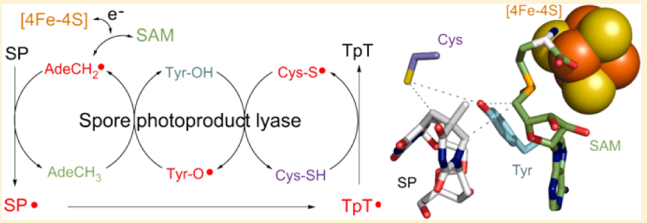

5-Thyminyl-5,6-dihydrothymine, commonly called spore photoproduct or SP, is the exclusive DNA photolesion identified in bacterial endospores.[1−3] SP accumulates in the bacterial sporulation phase and is repaired rapidly in the early germination phase, thus posing little threat to bacterial survival. The key enzyme responsible for SP repair is spore photoproduct lyase (SPL).[1−3] SPL is a radical *S*-adenosyl-L-methionine (SAM) enzyme that utilizes the classic tricysteinate CX_3CX_2C motif to bind a [4Fe-4S] cluster. In the +1 oxidation state, the cluster donates an electron to SAM, to cleave the C5′−S bond associated with the sulfonium ion and generate a 5′-deoxyadenosyl radical (5′-dA$^{\bullet}$) and methionine.[4−15] This 5′-dA$^{\bullet}$ abstracts a H atom from SP to initiate the radical cascade reaction to restore TpT (Figure 1).[6,16]

Yang et al. recently showed that 5′-dA$^{\bullet}$ stereoselectively abstracts the $H_{6\text{-pro-R}}$ atom of SP (Figure 1);[13] the resulting SP radical then fragments to generate a 3′-thymine allylic radical. This radical abstracts a H atom from a protein residue to yield the repaired thymine pair, TpT. The source of this H atom has recently been proposed to be the C141 residue in *Bacillus subtilis* (*Bs*) SPL,[5,12−14] rather than the 5′-dA as proposed previously.[6,7] The new mechanism is strongly supported by crystal structures of wild-type (WT) and mutant SPL from *Geobacillus thermodenitrificans* (*Gt*) determined by Benjdia et al.[17] The structure shows that the distance between the methylene bridge of the dinucleoside SP and the conserved cysteine is 4.5 Å (Figure 2), which is close enough for the cysteine to be the direct H atom donor.[17] The sequence of $SPL_{(Gt)}$ is ∼77% identical to that of $SPL_{(Bs)}$, but $SPL_{(Gt)}$ exhibits a −1 sequence shift for the conserved amino acids.

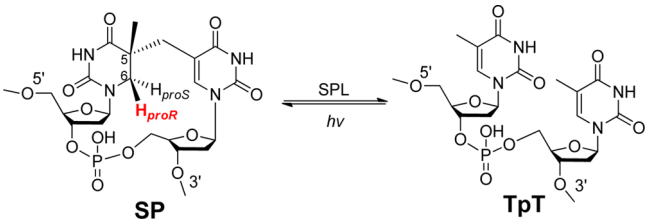

Figure 1. SP formation and enzymatic repair mediated by SPL. In this study, we also employed a d_4-SP TpT species, where the $H_{pro\text{-}R}$ atom and the three hydrogen atoms of the methyl group on the 5′-T are replaced by deuterium atoms.

Received: December 3, 2012
Revised: April 12, 2013

   dx.doi.org/10.1021/bi3016247 | *Biochemistry* XXXX, XXX, XXX−XXX

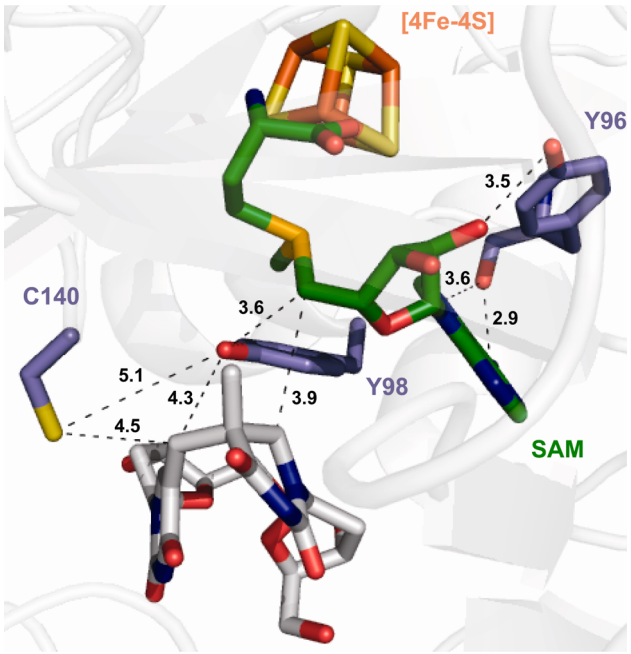

Figure 2. Active site of $SPL_{(Gt)}$ in complex with SP (white), the [4Fe-4S], cluster and SAM. The $C140_{(Gt)}$, $Y96_{(Gt)}$, and $Y98_{(Gt)}$ residues correspond to the $C141_{(Bs)}$, $Y97_{(Bs)}$, and $Y99_{(Bs)}$ residues in to $SPL_{(Bs)}$, respectively. The distances between protein residues, SP, and SAM are indicated by dashed lines (Protein Data Bank entry 4FHD).[17]

Previous work showed that SP repair by the SPL $C141A_{(Bs)}$ mutant results in the formation of $TpTSO_2^-$ as the major product and TpT as the minor one.[12] Because neither the equivalent mutation [$C140A_{(Gt)}$] nor the isosteric $C140S_{(Gt)}$ mutation changes the *Gt* SPL structure,[17] Benjdia et al. concluded that removal of the cysteine disturbs the H atom back-donation process during SPL catalysis.[17] Enzyme kinetic studies of the SPL $C141A_{(Bs)}$ mutant further demonstrate that both products form simultaneously, indicating that the conserved cysteine must be the intrinsic H atom donor to the substrate radical.[14] Such a H atom transfer (HAT) process leaves a thiyl radical on this cysteine. As SAM is suggested to be regenerated at the end of each catalytic cycle,[6,13] the thiyl radical must be involved in this regeneration process. Here we present experimental evidence to suggest that besides the cysteine, a couple of tyrosines are also essential for catalysis.

MATERIALS AND METHODS

General. The DNA-modifying enzymes were purchased from Fermentas Life Sciences (Glen Burnie, MD). Oligonucleotide primers were obtained from either Integrated DNA Technologies (Coralville, IA) or Eurofins MWG operon. *Escherichia coli* BL21(DE3) and expression vector pET-28a were purchased from Novagen (Madison, WI). The construct containing the $SPL_{(Bs)}$ gene was co-expressed with plasmid pDB1282, which was a generous gift from S. Booker at The Pennsylvania State University (University Park, PA). 5′-Deoxyadenosine (5′-dA) and SAM were purchased from Aldrich and used without further purification. All other buffers and chemicals were of the highest grade available.

Construction of the SPL Mutant Expression Vectors. The *splB* gene was cloned from the *Bs* chromosomal DNA (strain 168) into the in pET-28a vector with an N-terminal His_6 tag as previously described.[13] Site-directed mutagenesis was performed to obtain the desired mutations with the QuickChange site-directed mutagenesis kits from Stratagene using the manufacturer's instructions. The synthetic oligonucleotide primers that were used are listed in Table S1 of the Supporting Information. The constructs were transformed into *E. coli* 10 G chemically competent cells purchased from Lucigen Corp. (Middleton, WI) for isolation and amplification of the resulting plasmid DNA. The resulting vectors were then cotransformed with the pDB1282 vector into *E. coli* BL21-(DE3) for protein overexpression as described previously.[13] The $Y98F_{(Gt)}$ mutant used for the crystal structure derives from the *GTNG_2348* gene encoding SPL from *G. thermodenitrificans*. Site-directed mutagenesis was performed by QuickChange polymerase chain reaction mutagenesis using plasmid pETM11-His-tag-SPL as previously described,[17] and the primers are listed in Table S1 of the Supporting Information.

Expression and Purification of SPL Mutants. Both the WT enzyme and the tyrosine mutants for $SPL_{(Bs)}$ were expressed in lysogeny broth (LB) medium containing the appropriate antibiotics as previously described.[13] The proteins were purified via Ni-NTA chromatography followed by ion exchange chromatography using the SP-Sepharose fast flow ion exchange resin (GE Healthcare Life Sciences, Piscataway, NJ). The bound protein was washed using a buffer containing 25 mM Tris, 250 mM NaCl, and 10% glycerol (pH 7.0) for 10 column volumes. The protein was then eluted using the same buffer containing 500 mM NaCl instead. The resulting protein was diluted by 2-fold to reduce the salt concentration to 250 mM and saved for activity studies.

The expression and purification conditions used for the SPL $Y98F_{(Gt)}$ mutant protein were similar to those used for the WT enzyme.[17] The harvested cells were resuspended in buffer A [50 mM Tris-HCl (pH 8), 500 mM NaCl, 10 mM $MgCl_2$, and 10% glycerol] supplemented with 5 mM 2-mercaptoethanol, 1 tablet of protease inhibitor cocktail (Complete, EDTA-free, Roche), 4 μg/mL DNase I (Roche), 4 μg/mL RNase (Roche), and 0.1 mg/mL lysozyme (Sigma-Aldrich) and disrupted by sonication. After ultracentrifugation, the supernatant was loaded on a Ni-NTA (Qiagen) gel column equilibrated with buffer A containing 20 mM imidazole (Sigma-Aldrich). The mutant protein was eluted with 500 mM imidazole, which was then removed by a desalting column (Sephadex G-25, GE Healthcare). The SPL $Y98F_{(Gt)}$ protein was further purified by heparin affinity column chromatography (GE Healthcare) using 50 mM Tris-HCl (pH 8), 300 mM NaCl, 1% glycerol, and 3 mM dithiothreitol as the initial buffer.

Protein, Iron, and Sulfide Assays. Routine determinations of protein concentration were conducted by the Bradford method,[18] using bovine γ-globulin as the protein standard. Protein concentrations were calibrated on the basis of the absorption of aromatic residues at 280 nm in the presence of 6 M guanidine hydrochloride using the method of Gill and von Hippel.[19] The iron content was determined using *o*-bathophenanthroline (OBP) under reductive conditions after protein digestion in 0.8% $KMnO_4$ and 1.2 M HCl as described by Fish.[20] Sulfide assays were conducted using the method described by Beinert.[21]

Enzyme Activity Assay. Typically, a reaction mixture contained 30 μM $SPL_{(Bs)}$ enzyme (or tyrosine mutant), the corresponding SP TpT substrate (1 mM), and 150 μM SAM in a final volume of 400 μL of buffer containing 25 mM Tris-HCl, 300 mM NaCl, and 10% glycerol (pH 7.0). Sodium dithionite (final concentration of 1 mM) was added as a reductant to

dx.doi.org/10.1021/bi3016247 | *Biochemistry* XXXX, XXX, XXX–XXX

initiate the enzyme reaction. The reactions were conducted under anaerobic conditions at ambient temperature for various periods of time. Under the conditions of the assay, the formation of TpT was linear with time for up to 15 min. At each time point, 90 μL of the solution was taken out to an Eppendorf tube and quenched with 10 μL of 3 M HCl. After the protein residues had been removed via centrifugation at 15000 rpm for 20 min, the resulting supernatants were loaded onto a high-performance liquid chromatography (HPLC) instrument, separated, and analyzed via the procedure described previously.[13]

Deuterium Kinetic Isotope Effects (KIEs). The apparent (^{D}V) KIEs for the WT SPL$_{(Bs)}$ and C141A$_{(Bs)}$ mutant were reported in our previous publications.[13,14] The apparent KIEs for both Y-to-F mutants were determined in a similar manner by direct comparison of the initial rates with 1 mM SP TpT and d_4-SP TpT.[22] As pointed out by Cleland, this is the only method for apparent KIE determination for enzyme reactions.[23]

There are three possible procedures for determining the competitive [$^{D}(V/K)$] KIE, comparison of reciprocal plots with labeled and unlabeled substrates, internal competition, and equilibrium perturbation.[23,24] As shown previously, we were unable to obtain a meaningful reciprocal plot because of the extremely low enzyme activity using the dinucleotide SP TpT at a low substrate concentration.[13] The perturbation experiment works only for reactions that are readily reversible;[23,24] such a requirement is obviously not fulfilled in our SP repair reaction. Therefore, we adopted the internal competition approach, measuring the competitive KIE with an equimolar mixture of SP TpT and d_4-SP TpT (total concentration of 1 mM). The reaction was quenched by addition of HCl at different time points; the amount of TpT formed was determined by HPLC, and the deuterium content of the resulting TpT was subsequently determined by ESI-MS using the Agilent 6520 Accurate-Mass Q-TOF LC/MS spectrometer. The data were acquired via Agilent MassHunter Workstation Data Acquisition (B.03.00) and analyzed via Qualitative Analysis of MassHunter Acquisition Data (B.03.00).

At the steady state, the reaction rate can be described as[25]

$$v = (k_{cat}/K)[E][S]$$

Thus, for competing substrates

$$\frac{v_{SP}}{v_{d_4\text{-SP}}} = \frac{(k_{cat}/K)_{SP}[E][SP]}{(k_{cat}/K)_{d_4\text{-SP}}[E][d_4\text{-SP}]}$$

As $[SP]/[d_4\text{-SP}] = 1$

$$^{D}(V/K) = \frac{v_{SP}}{v_{d_4\text{-SP}}}$$

Therefore, the competitive KIE is reflected by the ratio between the two reaction rates when the concentrations of SP TpT and d_4-SP TpT are equal ($t = 0$). Because of the KIE, as the reaction progresses, the SP TpT and d_4-SP TpT concentrations are no longer the same. In our experiments, the KIEs at varying time points were measured at relatively low extents of reaction of between 1 and 10%. Under these conditions, the isotopic composition of the SPs varies approximately linearly with the extent of reaction. The competitive KIE was therefore calculated by linear extrapolation of the measured KIEs to a zero extent of reaction when the concentrations of SP TpT and d_4-SP TpT were equal (Figure S6 of the Supporting Information).[26]

One potential problem with such a treatment is the assumption that the enzyme reaction is at the steady state. Both the Y99F$_{(Bs)}$ and Y97F$_{(Bs)}$ mutants exhibit very short linear repair activities (one to two turnovers with the unlabeled substrate), which may bring uncertainty that the steady state hypothesis used above may not be valid. We therefore used a more general approach as defined by Cleland to re-examine the competitive KIEs from these internal competition reactions.[24] During the internal competition experiments, the $^{D}(V/K)$ can be calculated via the following formula:

$$^{D}(V/K) = \log[1 - f/(X_H + X_D R_p/R_0)] \Big/ \log[1 - f/(X_H + X_D R_0/R_p)]$$

where f is the fraction of the reaction for unlabeled SP TpT (d_4-SP TpT is treated as an inhibitor), R_0 ($\approx$1) is the mass ratio of starting substrates (SP TpT/d_4-SP TpT), R_p is the mass ratio of product at a fraction of the reaction, and X_H and X_D are initial mole fractions of unlabeled and deuterium-labeled substrates, respectively. In our experiments, both X_H and X_D equal 0.5.

f was determined by comparing the amount of TpT product obtained with the initial amount of unlabeled SP TpT substrate added. R_p can be readily determined by product analysis via ESI-MS. We thus recalculated the competitive KIEs and listed them in Table S3−S5 of the Supporting Information. These KIEs agree reasonably well with those determined under the steady state assumption. We therefore utilized the values determined via steady state kinetics for our discussions in this report.

EPR Experiments for *Bs* SPL and Its Mutants. Continuous wave (CW) EPR spectra of the SPL Y97A/Y99A$_{(Bs)}$ mutant were recorded on a modified Varian spectrometer at 35 GHz ("Q"-band) and 2 K.[27] The as-isolated mutant (300 μM, 3.0 irons/protein) was reduced with 2 mM sodium dithionite inside the anaerobic chamber for 0.5 h, transferred to the EPR tube, and immediately frozen in liquid N_2. The EPR spectra were recorded as described previously.[13] The EPR simulations performed using QPOW[28] as modified by J. Telser. The EPR samples for WT SPL$_{(Bs)}$, Y97F$_{(Bs)}$, and Y99F$_{(Bs)}$ were prepared in the anaerobic chamber by loading 200 μL of protein (~200 μM), which was reduced with 2 mM sodium dithionite for 0.5 h, into 4 mm outside diameter quartz tubes (Wilmad). The samples were frozen in liquid N_2 and shipped with a cryoshipper. EPR spectra were recorded on a Bruker E580 spectrometer using an ER4116DM dual-mode resonator in perpendicular mode, resonating at 9.633 GHz (X-band). The spectra were recorded at 10 K using an in-cavity liquid helium flow cooling system (Oxford ESR900 cryostat, Oxford ITC503S temperature controller). The microwave power was 1 mW, well below the estimated half-saturation power of 10 mW (data not shown). Further experimental parameters were as follows: modulation amplitude of 1 mT, modulation frequency of 100 kHz, sweep rate of 1.2 mT/s, and 11 (WT) and 7 [Y99F$_{(Bs)}$ and Y97F$_{(Bs)}$] scans.

Crystallization and Structural Determination of the SPL Y98F$_{(Gt)}$ Mutant. The purified SPL Y98F$_{(Gt)}$ protein was concentrated (30000 molecular weight cutoff spin concentrator, Amicon, Millipore). The iron−sulfur cluster was reconstituted under anaerobic conditions in a glovebox (Belle), after which the mutant protein was applied on a desalting column. As for WT SPL$_{(Gt)}$, crystals of the substrate-free Y98F$_{(Gt)}$ mutant grew

dx.doi.org/10.1021/bi3016247 | *Biochemistry* XXXX, XXX, XXX−XXX

Table 1. Summary of the *Bs* SPL Reactions

SPL enzyme	v (min^{-1})	apparent KIE[a]	competitive KIE[a]	repaired SP/5′-dA
WT	0.41 ± 0.03	2.8 ± 0.3	3.4 ± 0.3	1.5 ± 0.2
$C141A_{(Bs)}$	0.14 ± 0.02	1.7 ± 0.2	3.0 ± 0.3	1.08 ± 0.1
$Y97A/Y99A_{(Bs)}$	NA[b]	NA[b]	NA[b]	NA[b]
$Y97F_{(Bs)}$	0.12 ± 0.01	16 ± 1.5	11.5 ± 1.5	1.6 ± 0.2
$Y99F_{(Bs)}$	0.06 ± 0.005	10.5 ± 1	9 ± 1	1.0 ± 0.1
$Y97F/Y99F_{(Bs)}$	<0.004	NA[b]	NA[b]	0.92 ± 0.1

[a]As shown by Figures S5 and S6 of the Supporting Information, both KIEs were determined within the first three turnovers, where the steady state kinetics may not be achieved. [b]Not available.

in a hanging drop vapor diffusion setup using 70 mM octanoyl *N*-hydroxyethylglucamide (Hampton Research), 200 mM lithium sulfate, 100 mM Tris-HCl (pH 9), and 19−27% (w/v) PEG 8000. Single crystals were harvested into a cryoprotectant containing 15% (v/v) ethylene glycol before being flash-cooled in liquid N_2 inside the glovebox. Diffraction data were collected at beamline PX-II of the Swiss Light Source. Data collection statistics are listed in Table S3 of the Supporting Information. The WT SPL structure was used to phase the $Y98F_{(Gt)}$ mutant structure by molecular replacement. Data were processed with XDS, and refinement of the $Y98F_{(Gt)}$ mutant was performed using REFMAC. The structure superposition was achieved with Coot using the SSM program and including all residues.

RESULTS AND DISCUSSION

As shown in Figure 2, a conserved tyrosine [$Y98_{(Gt)}$] is located between $C140_{(Gt)}$ and the bound SAM in the *Gt* SPL active site, suggesting that it is likely involved in SPL catalysis.[17] Furthermore, most radical SAM enzymes possess an aromatic residue Φ located around the third cysteine in the CXXXCXΦC radical SAM motif, which is thought to maintain the position of SAM in the enzyme binding pocket through several interactions.[17] The conserved Φ residue [$Y96_{(Gt)}$] is indeed involved in a weak hydrogen bonding interaction with SAM (Figure 2). We hence hypothesize that one or both of these tyrosine residues may act as a H atom relay between the thiyl radical and 5′-dA and are thus involved in the SAM regeneration process.

To test this hypothesis, we mutated both tyrosines to alanines in $SPL_{(Bs)}$. The resulting $Y97A/Y99A_{(Bs)}$ double mutant still contains an intact [4Fe-4S] cluster, as demonstrated by the characteristic UV absorption at 420 nm and the iron−sulfur content analysis.[22] After reduction by dithionite, the resulting $[4Fe\text{-}4S]^+$ cluster exhibited an EPR signal similar to that of the wild-type (WT) enzyme.[22] Thus, the Y → A double mutation did not affect the stability of the iron−sulfur cluster. However, incubating the Y → A double mutant with excess SAM and dinucleotide SP TpT under reducing conditions did not yield any TpT product during a 3 h reaction, long enough for multiple turnovers by the active enzyme.[13,14] This inactivity suggests that removing these tyrosines disrupts the interaction between the phenol ring of $Y97_{(Bs)}$ and the adenine ring of SAM, subsequently affecting SAM binding and/or reductive cleavage. Because the ring−ring interaction is conserved in the Y → F mutation, the SP repair reaction should not be affected in the $Y97F/Y99F_{(Bs)}$ double mutant. However, compared to the WT $SPL_{(Bs)}$ reaction, the Y → F double mutant reaction is at least 100-fold slower (Table 1).[13]

Compared to tyrosine, phenylalanine retains the aromatic ring but does not support the radical propagation reaction because of the loss of the OH moiety.[29,30] Should any tyrosine be involved in the radical reaction, the SPL catalysis−SAM regeneration process would be altered by the Y → F mutation. We thus constructed the $Y97F_{(Bs)}$ and $Y99F_{(Bs)}$ single mutations in $SPL_{(Bs)}$ and investigated their impacts on the SP repair reaction. The [4Fe-4S] cluster remains intact in these Y → F mutants, as proven by iron−sulfur content analysis and EPR spectroscopy.[22]

The resulting Y → F single mutants are able to repair SP in the presence of excess dithionite and SAM (Figure 3 and Table 1). However, the reaction rates are 3- and 7-fold lower for the $Y97F_{(Bs)}$ and $Y99F_{(Bs)}$ mutants, respectively, than for the WT enzyme,[13,14] but comparable to that of the $C141A_{(Bs)}$ mutant.[14] Under saturating substrate conditions (30-fold greater enzyme concentration), linear repair activity was observed during the first two to five turnovers for WT $SPL_{(Bs)}$, $C141A_{(Bs)}$, and $Y97F_{(Bs)}$; afterward, the linear response is lost, likely because of enzyme inactivation. No burst kinetics was observed for these enzymes. For the $Y99F_{(Bs)}$ mutant, the first turnover results in the fastest reaction and the reaction decelerates after that.[22] However, given the low activity of this mutant, it is difficult to conclude whether the observed reduction in rate is due to enzyme inactivation or pre-steady state kinetics. All reactions decelerate when d_4-SP TpT, which has the $H_{6\text{-pro-R}}$ position

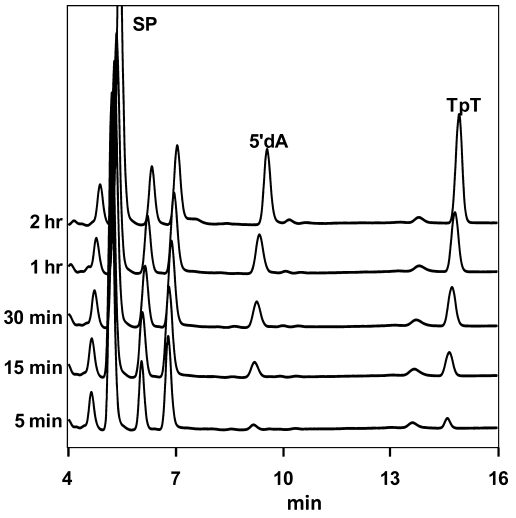

Figure 3. HPLC chromatograph of SP TpT repair mediated by the SPL $Y99F_{(Bs)}$ mutant with 30 μM enzyme, 150 μM SAM, and 1 mM dithionite. SP TpT eluted at 5.4 min, 5′-dA at 8.9 min, and TpT at 14.7 min. See the Supporting Information for the HPLC chromatograph of the $Y97F_{(Bs)}$ mutant reaction.

dx.doi.org/10.1021/bi3016247 | *Biochemistry* XXXX, XXX, XXX−XXX

deuterated (Figure 1), is used as a substrate. Comparing the initial reaction rates using the unlabeled SP and d_4-SP TpT as substrates gives us the traditional ^{D}V KIE.[23] Given the very short "steady state" for our enzyme reactions, all ^{D}V KIEs were determined within the first two enzyme turnovers except for that of the Y99F$_{(Bs)}$ mutant, which was determined within the first turnover; thus, we term the derived ^{D}V KIEs apparent KIEs. Analyzing the ratio of TpT to d_3-TpT (the abstracted deuterium is washed out during catalysis[13]) via mass spectroscopy results in the $^{D}(V/K)$ KIE, which is termed the competitive KIE in our discussion.

Theoretical calculations suggest that in the WT SPL reaction, both H atom abstraction steps associated with 5′-dA (5′-dA formation and 5′-dA$^{\bullet}$ regeneration) have high energy barriers.[31,32] Between them, it is more difficult to take a H atom from 5′-dA, indicating that 5′-dA$^{\bullet}$ regeneration is likely the rate-limiting (irreversible) step.[31] All previous steps, including the abstraction of a H atom from SP to form 5′-dA, belong to the "rate-determining zone"[33] and contribute to the rate-determining process.[34] Thus, the intrinsic deuterium isotope effect associated with abstraction of a H atom from d_4-SP TpT could be weakened by the subsequent catalytic steps. These computations consider SAM to be regenerated after each catalytic cycle,[31,32] as indicated by a previous experimental finding that using SP containing plasmid DNA, one molecule of SAM was thought to support >500 turnovers.[6] However, with the dinucleotide SP TpT as the substrate, one SAM molecule is found to support only 1.5 turnovers in our WT SPL$_{(Bs)}$ reaction probably because of the weak affinity of the substrate for the enzyme.[14] This result suggests that roughly two-thirds of the formed 5′-dA and methionine molecules exchange with the excess of SAM from the environment during SPL catalysis. Although there are no data describing how fast this exchange step is, the fact that the competitive KIE (3.4 ± 0.3) is slightly higher than the apparent KIE (2.8 ± 0.3) for WT SPL$_{(Bs)}$ indicates that the SAM binding or product release steps are also involved in the rate-limiting process.[34] As the reaction rates we observed are the average of two reactions, with one involving SAM regeneration and the other including exchange of SAM with 5′-dA, these numbers are unlikely to represent the true ^{D}V and $^{D}(V/K)$ KIEs that resulted from SP-containing oligomeric DNA. Therefore, although important mechanistic insight can still be obtained from our KIE studies, a systematic data analysis using mathematical models is difficult to perform because of the very complicated reaction process in our system.

Similar results were obtained for the C141A$_{(Bs)}$ mutant reaction. Compared with that of the WT SPL reaction, the apparent KIE is reduced to 1.7 ± 0.2. Furthermore, the competitive KIE is determined to be 3.0 ± 0.2, which is also smaller than that for WT SPL$_{(Bs)}$.[14] We tentatively ascribe the reduced KIEs to the slower radical quenching step caused by the removal of the intrinsic H atom donor on the protein.[14] Additionally, disruption of the putative catalytic chain indicates that SAM regeneration no longer occurs; all formed 5′-dA has to be exchanged with SAM at the end of a turnover, which contrasts to the two-thirds exchange ratio observed for the WT enzyme. Therefore, if the exchange process between 5′-dA and SAM is sufficiently slow to change the reaction energy profile, it will also contribute to the reduced KIEs exhibited by the C141A$_{(Bs)}$ mutant. On the other hand, the competitive KIEs for WT SPL$_{(Bs)}$ and C141A$_{(Bs)}$ are both larger than their respective apparent KIEs, suggesting that the SAM binding and 5′-dA release processes are similar in these two proteins.

As indicated in Figure 2, the [4Fe-4S] cluster in SPL restricts Y96$_{(Gt)}$ [Y97$_{(Bs)}$] from directly participating in radical transfer processes via ligation to C98, the third cysteine in the radical SAM motif. The SPL crystal structure identified Y97$_{(Bs)}$ as the Φ residue in the radical SAM motif,[35] likely playing a structural role to ensure the correct orientation of SAM as well as subsequent 5′-dA/5′-dA$^{\bullet}$ intermediates for an efficient catalysis. Such a function can be readily fulfilled by a phenylalanine residue. Indeed, Y, F, H, and W have all been found to serve as the Φ residue in other radical SAM enzymes.[35,36] Thus, the >3-fold reduction in rate exhibited by the Y97F$_{(Bs)}$ mutant (Table 1) is surprising. Moreover, the apparent KIE is changed to 16 ± 1.5 and the competitive KIE to 11.5 ± 1.5, which are much larger than the respective KIEs exhibited by WT SPL. These observations may be explained by altered interaction of residue Y97$_{(Bs)}$ with SAM after the Y → F mutation. A specific possibility is the loss of the interaction between the -OH moiety in Y97F$_{(Bs)}$ and the 2′-OH at the SAM ribose. Alternatively, these results suggest that although the crystal structure indicates that Y97$_{(Bs)}$ is not a direct component of the HAT chain, it not only may be involved in SAM binding but also may play other roles in enzyme catalysis (also see discussions below).

The SPL structure indicates that Y98$_{(Gt)}$ [equivalent to Y99$_{(Bs)}$] may be a direct component of the HAT chain, which is also confirmed by our kinetic data. Mutating Y99$_{(Bs)}$ in SPL to a phenylalanine results in a 7-fold reduced catalytic rate. Additionally, the Y99F$_{(Bs)}$ mutant exhibits an apparent KIE of 10.5 ± 1 and a competitive KIE of 9 ± 1, both of which are similar to the KIEs shown by the Y97F$_{(Bs)}$ mutant, but much higher than those of WT SPL$_{(Bs)}$ and C141A$_{(Bs)}$. These high KIEs also suggest that hydrogen tunneling may occur in this HAT step.[37,38] Moreover, the competitive KIEs are lower than the apparent KIEs in both Y97F$_{(Bs)}$ and Y99F$_{(Bs)}$ reactions, which is in contrast to the trend exhibited by WT SPL$_{(Bs)}$ and C141A$_{(Bs)}$, indicating that the SAM binding and 5′-dA release steps have been disturbed by these Y → F mutations.

The high KIEs exhibited by these Y → F mutants are accompanied by much enhanced uncoupled SAM cleavage reactions. As shown in Figure 4, when d_4-SP was used as the substrate, both WT SPL$_{(Bs)}$ and C141A$_{(Bs)}$ led to ∼10% of uncoupled SAM cleavage, as reflected by the small amount of unlabeled 5′-dA observed. In contrast, production of the unlabeled 5′-dA was enhanced ∼5-fold in the Y97F$_{(Bs)}$ or Y99F$_{(Bs)}$ mutant reaction, with a yield comparable to that of d_1-5′-dA, the product of abstraction of a H atom from d_4-SP. This suggests that deuterium abstraction by 5′-dA$^{\bullet}$ becomes unfavorable, which is in line with the high isotope effect observed in both mutants. As a consequence, ∼50% of the 5′-dA$^{\bullet}$ is quenched by reductants from the environment. The enhanced uncoupled SAM cleavage reaction in these Y → F mutants implies that the protein local conformation is essential for an efficient SPL catalysis. Cleavage of the strong C5′−S bond in SAM is assisted by the protein network in the rapid quenching of the resulting 5′-dA$^{\bullet}$, allowing a quick and efficient SP repair reaction in a synergistic manner.

Such a rationale also suggests that the rate-determining zone (or the first irreversible step) in Y97F$_{(Bs)}$ and Y99F$_{(Bs)}$ mutants may be different from that in the WT SPL$_{(Bs)}$ enzyme. As shown in radical SAM enzymes BtrN and DesII, the hydrogen atom abstraction step between the 5′-dA radical and the enzyme substrate is reversible as indicated by the multiple deuterium transfers from the labeled substrate to 5′-dA or

dx.doi.org/10.1021/bi3016247 | Biochemistry XXXX, XXX, XXX−XXX

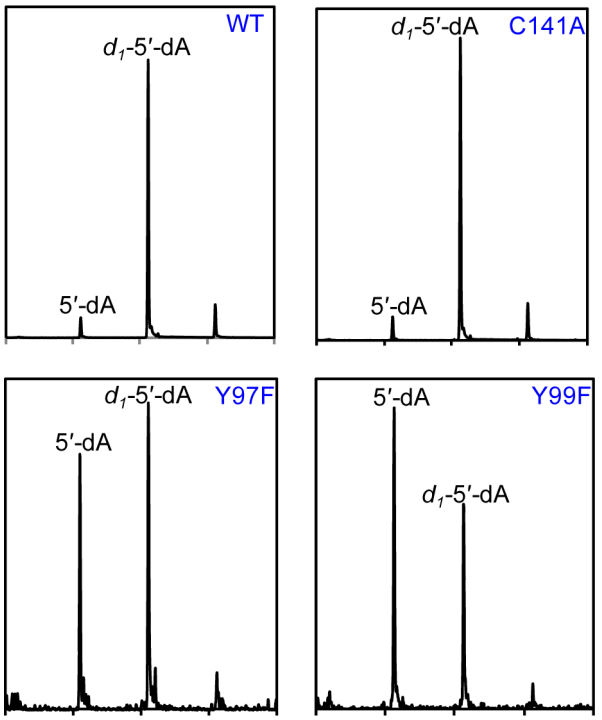

Figure 4. Mass spectrometry analysis of 5′-dA isolated from *Bs* SPL reactions conducted with d_4-SP TpT as the substrate. d_1-5′-dA forms via abstraction of a H atom from d_4-SP TpT, and the unlabeled 5′-dA forms via uncoupled SAM cleavage. The exact mass for each 5′-dA species is given in the Supporting Information.

SAM.[39,40] Although a similar multiple-deuterium transfer was not observed in SPL catalysis probably because of the poor binding affinity for the dinucleotide SP TpT substrate, the low extent of uncoupled SAM cleavage reaction in WT $SPL_{(Bs)}$ suggests that this step is facilitated by the protein network and thus could very well be reversible. Therefore, in the WT $SPL_{(Bs)}$ enzyme, the rate-determining zone likely ends at the H atom abstraction step to produce the 5′-dA radical for SAM regeneration. In contrast, the enhanced uncoupled cleavage in the two Y → F mutants suggests that the first H atom abstraction associated with SP is no longer a favorable step, making it highly unlikely to be reversible. Therefore, it is possible that the rate-determining zone may include only SAM/SP TpT binding, SAM reductive cleavage, and the H atom abstraction step for these Y → F mutants. As a consequence, much larger apparent and competitive KIEs have been observed.

To exclude any effect of the $Y99F_{(Bs)}$ mutation on the protein structure, we determined the crystal structure of the corresponding $Y98F_{(Gt)}$ mutant in *Gt* SPL to 2.3 Å resolution. Comparison of the substrate-free $Y98F_{(Gt)}$ mutant with the structure of the WT enzyme confirms the structural integrity of the mutant protein and shows a conserved conformation with an overall root-mean-square deviation of 0.15 Å for the superimposed protein backbone (Figure 5). A more magnified view of the $Y98F_{(Gt)}$ mutant active site shows that its overall architecture and the interactions between the protein and SAM are highly similar to those of the WT enzyme.[17] In particular, the phenylalanine backbone superposes well with the WT tyrosine. WT $SPL_{(Gt)}$ and $Y98F_{(Gt)}$ repair SP TpT at reaction rates of 0.32 and 0.04 min^{-1}, respectively, both of which are comparable to those exhibited by the corresponding *Bs*

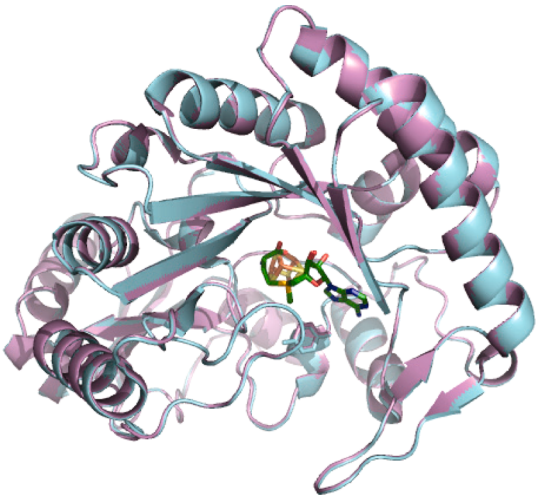

Figure 5. Secondary structure of substrate-free WT $SPL_{(Gt)}$ (cyan) and the $Y98F_{(Gt)}$ mutant [purple, equivalent to the $Y99F_{(Bs)}$ mutant Protein Data Bank entry 4K9R]. The superposition of both structures was performed with Coot using the SSM program and all residues.[65] The iron−sulfur cluster is colored orange (Fe) and yellow (S). SAM is colored by atom type (green for C, blue for N, red for O, and yellow for S). Y98 in the WT $SPL_{(Gt)}$ and F98 in the $Y98F_{(Gt)}$ mutant are depicted in stick format.

enzymes (Table 1). Moreover, these *Gt* enzymes display apparent KIEs identical to those of their *Bs* counterparts. Considering the ∼77% level of sequence identity between these two enzymes, we conclude that the structural information obtained for *Gt* SPL also reflects the *Bs* enzyme.

Both enzyme kinetics and the structural data suggest that the two tyrosine residues are involved in the SPL catalytic cycle. They must play a role downstream of $C141_{(Bs)}$, the intrinsic H atom donor, in the radical relay chain. We tentatively assign $Y99_{(Bs)}$ to be directly involved in the radical transfer in mediating SAM regeneration (Figure 6). Such a functional assignment is supported by the crystal structures of $SPL_{(Gt)}$. $Y98_{(Gt)}$ [equivalent of $Y99_{(Bs)}$] is located between C140 and SAM; its hydroxyl group is 5.1 Å from the SH moiety of C140 and 3.6 Å from the methylene carbon of SAM (Figure 2). Thus, it is potentially close to the 5′-dA moiety and well positioned for the radical relay process to mediate SAM regeneration. $Y99_{(Bs)}$ also helps stabilize the transient protein conformation right after the SAM cleavage reaction and thus allows a tightly coupled enzymatic reaction. C5′−S bond cleavage likely induces a subtle protein conformational change before 5′-dA$^{\bullet}$ attacks the $H_{6\text{-pro-R}}$ atom to initiate the SP repair process. This conformational change is disturbed in the $Y99F_{(Bs)}$ mutant, as indicated by the much enhanced uncoupled SAM cleavage (Figure 4). A similar impact on the protein transient conformation is also expected for the $Y97_{(Bs)}$ residue, as reflected by the enhanced uncoupled SAM cleavage in the $Y97F_{(Bs)}$ mutant reaction.

The tightly coupled radical relay mechanism is consistent with our experimental finding that no organic radical intermediate was observed by EPR spectroscopy in the steady state of the WT $SPL_{(Bs)}$-catalyzed SP TpT repair reaction. A similar observation was reported by Broderick et al. using SP-containing plasmid DNA as the enzyme substrate.[6] These observations contradict a recent report in which a UV−visible difference spectrum was suggested to correspond to the $^{\bullet}Y98_{(Gt)}$ radical formed during the $SPL_{(Gt)}$ steady state

dx.doi.org/10.1021/bi3016247 | *Biochemistry* XXXX, XXX, XXX−XXX

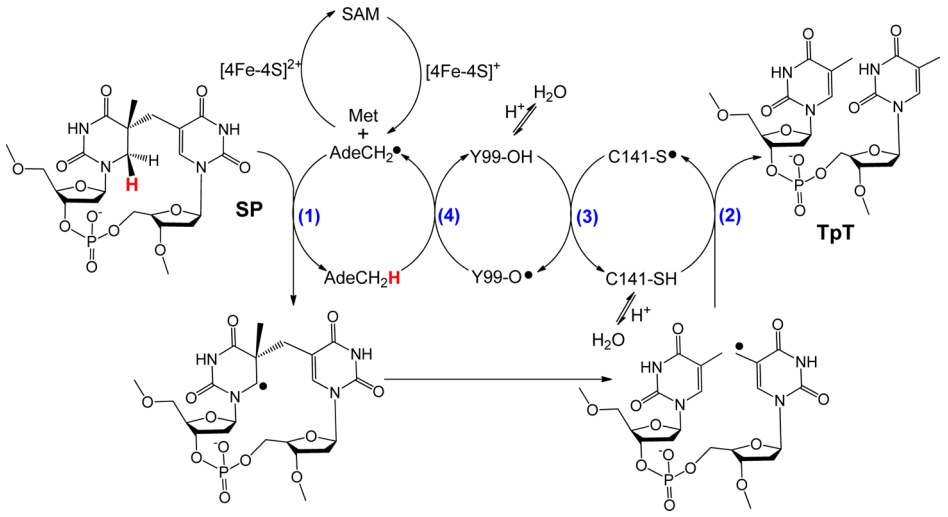

Figure 6. Hypothesized reaction mechanism for SPL (the residues are numbered according to the protein sequence in *Bs* SPL). This mechanism implies that SPL uses a minimum of four H atom transfer processes (labeled with blue numbers) in each catalytic cycle. One of the four processes occurs between a tyrosine and a cysteine, suggesting that SPL uses a novel HAT pathway for SAM regeneration. The role of $Y97_{(Bs)}$ in SPL catalysis needs further elucidation and is thus not shown here.

reaction.[15] However, that spectrum did not resemble the sharp-peak absorbance exhibited by a typical •Y.[41−44] We thus tentatively ascribe the cause of the spectral difference to the FeS chromophores, rather than to a tyrosyl radical. Among the possible reaction intermediates shown in Figure 6, the tyrosyl radical on $Y99_{(Bs)}$ is likely the most stable.[29,45] Stable tyrosyl radicals have been observed in a number of radical enzymes, including class I ribonucleotide reductase (RNR),[29,45,46] monoamine oxidase A,[47] photosystem II,[48] and prostaglandin H synthase (PGHS).[49,50] In addition, the thymine methyl radical must be reasonably stable as well, because of its position α to the thymine ring. The fact that no radical can be observed by EPR during the SPL steady state suggests these putative radical intermediates in Figure 6 exist as transient species. SPL catalysis likely occurs in a carefully regulated fashion: once the radical intermediate is generated via SAM reductive cleavage, it will be passed quickly through the catalytic chain until the end of the reaction and no radical species are accumulating during catalysis. This process is facilitated by transient protein conformational changes, preventing any of the intermediates from accumulating.

Although we have proposed SAM to be regenerated after each catalytic cycle, the obtained TpT/5′-dA ratios in the $SPL_{(Bs)}$ reactions are not fully in line with this hypothesis. As shown in Table 1, an ∼1/1 ratio was observed between the consumed SP TpT and the formed 5′-dA for both $C141A_{(Bs)}$[14] and $Y99F_{(Bs)}$ reactions, which is consistent with the assumption that these residues are components of the HAT chain for SAM regeneration. In contrast, the ratio is ∼1.5/1 in both WT $SPL_{(Bs)}$[13] and the $Y97F_{(Bs)}$ mutant, suggesting that only one-third of the SAM is regenerated here. We tentatively ascribe this discrepancy to the much weaker binding affinity of the dinucleotide SP TpT compared to that of the SP-containing duplex DNA. As indicated by DNA footprinting studies, $SPL_{(Bs)}$ protects at least a 9 bp region surrounding SP; all negatively charged phosphodiester moieties within this region are likely to contribute to the binding interaction with SPL.[51] A similar example can be found in DNA photolyase, which repairs the cyclobutane dimer in visible light. The photolyase recognizes 6 bp surrounding the dimer.[52] The binding affinity of the dinucleotide thymine dimer for photolyase is 10^4-fold lower than that of the dimer-containing oligonucleotide,[53] suggesting that loss of the extra electrostatic interactions via removal of the phosphodiester moieties upstream and downstream of the dimer drastically weakens binding of the substrate to the enzyme. Considering that $SPL_{(Bs)}$ recognizes three more phosphodiester groups than photolyase, the binding affinity of dinucleotide SP TpT is likely to be much weaker than that of the SP-containing duplex oligonucleotide. Therefore, d_4-SP-containing oligonucleotides will be needed to re-examine the KIEs reported here before the mechanism in Figure 6 can be fully established. Such experiments are not trivial considering the synthetic challenge in preparing enough deuterium-labeled SP-containing oligomers. On the other hand, despite the imperfect substrates used in the studies presented here, the obviously different reaction rates as well as the apparent and competitive KIEs among the WT and mutant SPL proteins still provide strong support for our proposed mechanism. The similar SAM regeneration pattern of the $Y97F_{(Bs)}$ mutant and WT $SPL_{(Bs)}$ also supports our hypothesis that $Y97_{(Bs)}$ may not be a direct component of the HAT pathway.

Another potential challenge to establishing our mechanism described above is the reasonable stability for the putative $•Y99_{(Bs)}$ species. The redox potential for a tyrosyl radical (0.94 V) is suggested to be 0.4 V lower than that of a cysteinyl radical (1.33 V) at pH 7.[29,45] Moreover, the bond dissociation energy (BDE) is found to be 360 kJ/mol for the O−H bond in tyrosine and 368−381 kJ/mol for the S−H bond in cysteine,[29,45] although some recent calculations suggest that the BDEs for the tyrosyl O−H and cysteinyl S−H bonds are very similar (365 ± 5 kJ/mol).[32] Nevertheless, considering the strong C−H bond in 5′-dA, which possesses a BDE of 433 kJ/mol,[54,55] the last H atom abstraction step (step 4 in Figure 6) to regenerate the 5′-dA• in our mechanism is therefore strongly uphill. Among the enzymatic reactions studied to date, the case most similar to our mechanistic proposal is probably the adenosylcob(II)alamin regeneration in class II RNR. Class II RNR utilizes an adenosylcob(II)alamin coupled by a conserved cysteine for catalysis.[45,56] The catalytically essential cysteinyl radical is suggested to take a H atom from the methyl moiety of

dx.doi.org/10.1021/bi3016247 | *Biochemistry* XXXX, XXX, XXX−XXX

5′-dA, producing the 5′-dA• radical that recombines with cob(III)alamin to regenerate the cofactor at the end of each catalytic cycle. This thermodynamically unfavorable H atom abstraction is considered to be coupled with the favorable adenosylcob(II)alamin regeneration step. SAM regeneration is even more favored thermodynamically.[57] The C5′−S bond in SAM possesses a BDE of ∼251 kJ/mol,[36] indicating that it is much stronger than the C−Co bond in adenosylcobalamin, which exhibits a BDE of 134 kJ/mol.[58] Therefore, formation of the highly favorable C−S bond in SAM may compensate for the unfavorable H atom abstraction by the tyrosyl radical and allow the SAM regeneration step to proceed.

Although thermodynamically the regeneration of SAM is not an issue, the 70−80 kJ/mol BDE difference between the O−H bond in tyrosine and the C−H bond in 5′-dA suggests that kinetically this process is still slow. As shown by Frey et al., ligation of SAM to the [4Fe-4S] cluster in lysine 2,3-aminomutase (LAM) can lower the energy barrier for the SAM reductive cleavage step by almost 1 V (∼80 kJ/mol).[59] It is reasonable to assume that transition state stabilization via the protein environment may be available in SPL as well, making the energy barrier for this H atom abstraction step surmountable. Additionally, SAM regeneration may also be assisted by the $Y97_{(Bs)}$ residue. As discussed above, $Y97_{(Bs)}$ likely plays a key role in SAM/5′-dA• binding. However, we cannot rule out its further interaction with 5′-dA•, leading to $^{\bullet}Y97_{(Bs)}$. Such a hypothesis implies both $Y97_{(Bs)}$ and $Y99_{(Bs)}$ are involved in the radical propagation process, which may justify the similar high KIEs as well as the similarly enhanced uncoupled SAM cleavage reactions observed in $Y99F_{(Bs)}$ and $Y97F_{(Bs)}$ mutants. An example of this can be found in the PGHS enzyme, which catalyzes prostaglandin synthesis.[49,50] The cyclooxygenase reaction in PGHS employs a catalytically essential tyrosine radical, •Y385. However, another tyrosine, Y504, has also been identified as a radical carrier.[60] The •Y385 and •Y504 radicals are formed independently and appear to be in equilibrium after formation.[49] Y504 is proposed to serve as a reservoir of oxidizing equivalent, and the Y504F mutant decreases the cyclooxygenase activation efficiency by 50% for PGHS-1 and 200% for PGHS-2.[60] Recently, using the 3-nitrotyrosyl radical in place of •Y122 in *E. coli* class 1a RNR, Stubbe et al. showed that the radical is delocalized onto the three tyrosines of the long-range proton-coupled electron transfer pathway.[61] Y356 is the predominant location (85−90%) of the radical, with the remaining 10−15% delocalized onto Y731 and Y730 in subunit $\alpha 2$.[61] Such an observation also suggests that the relative redox potential between Y356 and Y731/730 could vary by ∼100 mV. Similarly, the involvement of $Y97_{(Bs)}$ may result in a partially populated •Y at this residue, which can interact and fine-tune the redox potential of the $^{\bullet}Y99_{(Bs)}$ and/or 5′-dA• radical. Such a radical delocalization likely reduces the energy barrier for the H atom abstraction step, making it kinetically competent. Further work to reveal the biological function of $Y97_{(Bs)}$ using X-ray crystallography and biochemical means is currently in progress.

In conclusion, our report strongly implicates SPL as the first member of the radical SAM superfamily to possibly bear a HAT chain. This transfer chain is likely to be essential for SAM regeneration in SPL catalysis. For the past decade, only SPL and LAM were considered to use SAM catalytically.[58,62] Very recently, another radical SAM enzyme, 7-carboxy-7-deazaguanine synthase (QueE), was found to recycle SAM after each turnover.[63] Considering the large number of radical SAM enzymes discovered to date (more than 44000[64]), a catalytic role of SAM can be expected among additional members of this superfamily. Our studies thus provide much-needed insight into understanding the SAM regeneration process not only in SPL but also potentially in other radical SAM enzymes.

■ ASSOCIATED CONTENT

Supporting Information

Experimental details and characterization data. This material is available free of charge via the Internet at http://pubs.acs.org.

■ AUTHOR INFORMATION

Corresponding Author

*A.B.: Department of Biomolecular Mechanisms, Max-Planck Institute for Medical Research, Jahnstrasse 29, 69120 Heidelberg, Germany; telephone, +49 6221 486 515; fax, +49 6221 486 585; e-mail, alhosna.benjdia@mpimf-heidelberg.mpg.de. S.S.: Department of Chemistry, University of Washington, Seattle, WA 98195; telephone, (206) 543-2906; e-mail, stst@uw.edu. L.L.: Department of Chemistry and Chemistry Biology, Indiana University-Purdue University Indianapolis, 402 N. Blackford Street, LD 326, Indianapolis, IN 46202; telephone, (317) 278-2202; fax, (317) 274-4701; e-mail, lilei@iupui.edu.

Author Contributions

L.Y., R.S.N., and A.B. contributed equally to this work.

Funding

This research is supported by the National Institutes of Health (R00ES017177) as well as the IUPUI startup fund (L.L.), the University of Washington (S.S.), the European Molecular Biology Organization (EMBO Long-Term fellowship) (A.B.), and the Max Planck Society (I.S.). The NMR and MS facilities at IUPUI are supported by National Science Foundation (NSF) MRI Grants CHE-0619254 and DBI-0821661, respectively. The EPR facilities at Northwestern University are funded by NSF Grant MCB-0316038.

Notes

The authors declare no competing financial interest.

■ ACKNOWLEDGMENTS

We thank Professors Bruce Palfey and Neil Marsh (University of Michigan, Ann Arbor, MI) and Professor J. Martin Bollinger (The Pennsylvania State University) for helpful discussions on steady state enzyme kinetics and KIE determination. We also thank Professor JoAnne Stubbe (Massachusetts Institute of Technology, Cambridge, MA) for her insightful comments about the SAM regeneration process in SPL catalysis. We thank Professor Brian M. Hoffman (Northwestern University, Evanston, IL) for use of the 35 GHz EPR spectrometer. We thank the Dortmund-Heidelberg team for data collection at the Swiss Light Source, beamline X10SA (Paul Scherrer Institute, Villigen, Switzerland).

■ REFERENCES

(1) Setlow, P. (2006) Spores of *Bacillus subtilis*: Their resistance to and killing by radiation, heat and chemicals. *J. Appl. Microbiol. 101*, 514−525.

(2) Desnous, C. L., Guillaume, D., and Clivio, P. (2010) Spore photoproduct: A key to bacterial eternal life. *Chem. Rev. 110*, 1213−1232.

(3) Li, L. (2012) Mechanistic studies of the radical SAM enzyme spore photoproduct lyase (SPL). *Biochim. Biophys. Acta 1824*, 1264−1277.

(4) Rebeil, R., and Nicholson, W. L. (2001) The subunit structure and catalytic mechanism of the *Bacillus subtilis* DNA repair enzyme spore photoproduct lyase. *Proc. Natl. Acad. Sci. U.S.A. 98*, 9038−9043.
(5) Fajardo-Cavazos, P., Rebeil, R., and Nicholson, W. (2005) Essential cysteine residues in *Bacillus subtilis* spore photoproduct lyase identified by alanine scanning mutagenesis. *Curr. Microbiol. 51*, 331−335.
(6) Cheek, J., and Broderick, J. (2002) Direct H atom abstraction from spore photoproduct C-6 initiates DNA repair in the reaction catalyzed by spore photoproduct lyase: Evidence for a reversibly generated adenosyl radical intermediate. *J. Am. Chem. Soc. 124*, 2860−2861.
(7) Buis, J., Cheek, J., Kalliri, E., and Broderick, J. (2006) Characterization of an active spore photoproduct lyase, a DNA repair enzyme in the radical *S*-adenosylmethionine superfamily. *J. Biol. Chem. 281*, 25994−26003.
(8) Chandra, T., Silver, S. C., Zilinskas, E., Shepard, E. M., Broderick, W. E., and Broderick, J. B. (2009) Spore photoproduct lyase catalyzes specific repair of the 5*R* but not the 5*S* spore photoproduct. *J. Am. Chem. Soc. 131*, 2420−2421.
(9) Silver, S., Chandra, T., Zilinskas, E., Ghose, S., Broderick, W., and Broderick, J. (2010) Complete stereospecific repair of a synthetic dinucleotide spore photoproduct by spore photoproduct lyase. *J. Biol. Inorg. Chem. 15*, 943−955.
(10) Pieck, J., Hennecke, U., Pierik, A., Friedel, M., and Carell, T. (2006) Characterization of a new thermophilic spore photoproduct lyase from *Geobacillus stearothermophilus* (SplG) with defined lesion containing DNA substrates. *J. Biol. Chem. 281*, 36317−36326.
(11) Chandor, A., Berteau, O., Douki, T., Gasparutto, D., Sanakis, Y., Ollagnier-De-Choudens, S., Atta, M., and Fontecave, M. (2006) Dinucleotide spore photoproduct, a minimal substrate of the DNA repair spore photoproduct lyase enzyme from *Bacillus subtilis*. *J. Biol. Chem. 281*, 26922−26931.
(12) Chandor-Proust, A., Berteau, O., Douki, T., Gasparutto, D., Ollagnier-De-Choudens, S., Fontecave, M., and Atta, M. (2008) DNA repair and free radicals, new insights into the mechanism of spore photoproduct lyase revealed by single amino acid substitution. *J. Biol. Chem. 283*, 36361−36368.
(13) Yang, L., Lin, G., Liu, D., Dria, K. J., Telser, J., and Li, L. (2011) Probing the reaction mechanism of spore photoproduct lyase (SPL) via diastereoselectively labeled dinucleotide SP TpT substrates. *J. Am. Chem. Soc. 133*, 10434−10447.
(14) Yang, L., Lin, G., Nelson, R. S., Jian, Y., Telser, J., and Li, L. (2012) Mechanistic studies of the spore photoproduct lyase via a single cysteine mutation. *Biochemistry 51*, 7173−7188.
(15) Kneuttinger, A. C., Heil, K., Kashiwazaki, G., and Carell, T. (2013) The radical SAM enzyme spore photoproduct lyase employs a tyrosyl radical for DNA repair. *Chem. Commun. 49*, 722−724.
(16) Mehl, R. A., and Begley, T. P. (1999) Mechanistic studies on the repair of a novel DNA photolesion: The spore photoproduct. *Org. Lett. 1*, 1065−1066.
(17) Benjdia, A., Heil, K., Barends, T. R. M., Carell, T., and Schlichting, I. (2012) Structural insights into recognition and repair of UV-DNA damage by spore photoproduct lyase, a radical SAM enzyme. *Nucleic Acids Res. 40*, 9308−9318.
(18) Bradford, M. M. (1976) A rapid and sensitive method for the quantitation of microgram quantities of protein utilizing the principle of protein-dye binding. *Anal. Biochem. 72*, 248−254.
(19) Gill, S. C., and Von Hippel, P. H. (1989) Calculation of protein extinction coefficients from amino acid sequence data. *Anal. Biochem. 182*, 319−326.
(20) Fish, W. W. (1988) Rapid colorimetric micromethod for the quantitation of complexed iron in biological samples. *Methods Enzymol. 158*, 357−364.
(21) Beinert, H. (1983) Semi-micro methods for analysis of labile sulfide and of labile sulfide plus sulfane sulfur in unusually stable iron-sulfur proteins. *Anal. Biochem. 131*, 373−378.
(22) See the Supporting Information.
(23) Cleland, W. W. (2005) The use of isotope effects to determine enzyme mechanisms. *Arch. Biochem. Biophys. 433*, 2−12.
(24) Cleland, W. W. (2006) Enzyme mechanisms from isotope effects. In *Isotope effects in chemistry and biology* (Kohen, A., and Limbach, H.-H., Eds.) Chapter 37, pp 915−930, Taylor & Francis, Boca Raton, FL.
(25) Fersht, A. (1999) *Structure and mechanism in protein science: A guide to enzyme catalysis and protein folding*, Chapter 3, pp 103−131, W. H. Freeman and Co., New York.
(26) Li, L., and Marsh, E. N. G. (2006) Deuterium isotope effects in the unusual addition of toluene to fumarate catalyzed by benzylsuccinate synthase. *Biochemistry 45*, 13932−13938.
(27) Werst, M. M., Davoust, C. E., and Hoffman, B. M. (1991) Ligand spin densities in blue copper proteins by Q-band ^{1}H and ^{14}N ENDOR spectroscopy. *J. Am. Chem. Soc. 113*, 1533−1538.
(28) Belford, R. L., and Nilges, M. J. (1979) Computer simulations of powder spectra. In EPR Symposium, 21st Rocky Mountain Conference, Denver, CO.
(29) Stubbe, J., Nocera, D. G., Yee, C. S., and Chang, M. C. Y. (2003) Radical initiation in the class I ribonucleotide reductase: Long-range proton-coupled electron transfer? *Chem. Rev. 103*, 2167−2201.
(30) Jordan, A., and Reichard, P. (1998) Ribonucleotide reductases. *Annu. Rev. Biochem. 67*, 71−98.
(31) Guo, J., Luo, Y., and Himo, F. (2003) DNA repair by spore photoproduct lyase: A density functional theory study. *J. Phys. Chem. B 107*, 11188−11192.
(32) Hioe, J., and Zipse, H. (2010) Radicals in enzymatic catalysis: A thermodynamic perspective. *Faraday Discuss. 145*, 301−313.
(33) Yagisawa, S. (1989) Two types of rate-determining step in chemical and biochemical processes. *Biochem. J. 263*, 985−988.
(34) Northrop, D. B. (1975) Steady-state analysis of kinetic isotope effects in enzymic reactions. *Biochemistry 14*, 2644−2651.
(35) Vey, J. L., and Drennan, C. L. (2011) Structural insights into radical generation by the radical SAM superfamily. *Chem. Rev. 111*, 2487−2506.
(36) Frey, P., and Magnusson, O. (2003) S-Adenosylmethionine: A wolf in sheep's clothing, or a rich man's adenosylcobalamin? *Chem. Rev. 103*, 2129−2148.
(37) Kohen, A., and Klinman, J. P. (1998) Enzyme catalysis: Beyond classical paradigms. *Acc. Chem. Res. 31*, 397−404.
(38) Kohen, A., and Klinman, J. P. (1999) Hydrogen tunneling in biology. *Chem. Biol. 6*, R191−R198.
(39) Yokoyama, K., Numakura, M., Kudo, F., Ohmori, D., and Eguchi, T. (2007) Characterization and mechanistic study of a radical SAM dehydrogenase in the biosynthesis of butirosin. *J. Am. Chem. Soc. 129*, 15147−15155.
(40) Szu, P.-H., Ruszczycky, M. W., Choi, S.-H., Yan, F., and Liu, H.-W. (2009) Characterization and mechanistic studies of DesII: A radical *S*-adenosyl-L-methionine enzyme involved in the biosynthesis of TDP-D-desosamine. *J. Am. Chem. Soc. 131*, 14030−14042.
(41) Cotruvo, J. A., Stich, T. A., Britt, R. D., and Stubbe, J. (2013) Mechanism of assembly of the dimanganese-tyrosyl radical cofactor of class Ib ribonucleotide reductase: Enzymatic generation of superoxide is required for tyrosine oxidation via a Mn(III)Mn(IV) intermediate. *J. Am. Chem. Soc. 135*, 4027−4039.
(42) Torrents, E., Sahlin, M., Biglino, D., Gräslund, A., and Sjöberg, B.-M. (2005) Efficient growth inhibition of *Bacillus anthracis* by knocking out the ribonucleotide reductase tyrosyl radical. *Proc. Natl. Acad. Sci. U.S.A. 102*, 17946−17951.
(43) Cotruvo, J. A., and Stubbe, J. (2011) *Escherichia coli* class Ib ribonucleotide reductase contains a dimanganese(III)-tyrosyl radical cofactor *in vivo*. *Biochemistry 50*, 1672−1681.
(44) Bollinger, J. M., Jr., Edmondson, D. E., Huynh, B. H., Filley, J., Norton, J. R., and Stubbe, J. (1991) Mechanism of assembly of the tyrosyl radical-dinuclear iron cluster cofactor of ribonucleotide reductase. *Science 253*, 292−298.
(45) Stubbe, J., and Van Der Donk, W. A. (1998) Protein radicals in enzyme catalysis. *Chem. Rev. 98*, 705−762.

(46) Cotruvo, J. A., and Stubbe, J. (2011) Class I ribonucleotide reductases: Metallocofactor assembly and repair *in vitro* and *in vivo*. *Annu. Rev. Biochem. 80*, 733−767.
(47) Rigby, S. E. J., Hynson, R. M. G., Ramsay, R. R., Munro, A. W., and Scrutton, N. S. (2005) A stable tyrosyl radical in monoamine oxidase A. *J. Biol. Chem. 280*, 4627−4631.
(48) Faller, P., Debus, R. J., Brettel, K., Sugiura, M., Rutherford, A. W., and Boussac, A. (2001) Rapid formation of the stable tyrosyl radical in photosystem II. *Proc. Natl. Acad. Sci. U.S.A. 98*, 14368−14373.
(49) Tsai, A.-L., and Kulmacz, R. J. (2010) Prostaglandin H synthase: Resolved and unresolved mechanistic issues. *Arch. Biochem. Biophys. 493*, 103−124.
(50) Lü, J.-M., Rogge, C. E., Wu, G., Kulmacz, R. J., Van Der Donk, W. A., and Tsai, A.-L. (2011) Cyclooxygenase reaction mechanism of PGHS: Evidence for a reversible transition between a pentadienyl radical and a new tyrosyl radical by nitric oxide trapping. *J. Inorg. Biochem. 105*, 356−365.
(51) Slieman, T. A., Rebeil, R., and Nicholson, W. L. (2000) Spore photoproduct (SP) lyase from *Bacillus subtilis* specifically binds to and cleaves SP (5-thyminyl-5,6-dihydrothymine) but not cyclobutane pyrimidine dimers in UV-irradiated DNA. *J. Bacteriol. 182*, 6412−6417.
(52) Sancar, A. (2003) Structure and function of DNA photolyase and cryptochrome blue-light photoreceptors. *Chem. Rev. 103*, 2203−2238.
(53) Kim, S. T., and Sancar, A. (1991) Effect of base, pentose, and phosphodiester backbone structures on binding and repair of pyrimidine dimers by *Escherichia coli* DNA photolyase. *Biochemistry 30*, 8623−8630.
(54) Hioe, J., Savasci, G., Brand, H., and Zipse, H. (2011) The stability of Cα peptide radicals: Why glycyl radical enzymes? *Chem.—Eur. J. 17*, 3781−3789.
(55) Hioe, J., and Zipse, H. (2012) Hydrogen transfer in SAM-mediated enzymatic radical reactions. *Chem.—Eur. J. 18*, 16463−16472.
(56) Licht, S., Gerfen, G. J., and Stubbe, J. (1996) Thiyl radicals in ribonucleotide reductases. *Science 271*, 477−481.
(57) Hinckley, G. T., and Frey, P. A. (2006) Cofactor dependence of reduction potentials for $[4Fe\text{-}4S]^{2+/1+}$ in lysine 2,3-aminomutase. *Biochemistry 45*, 3219−3225.
(58) Marsh, E. N. G., Patterson, D. P., and Li, L. (2010) Adenosyl radical: Reagent and catalyst in enzyme reactions. *ChemBioChem 11*, 604−621.
(59) Wang, S. C., and Frey, P. A. (2007) Binding energy in the one-electron reductive cleavage of *S*-adenosylmethionine in lysine 2,3-aminomutase, a radical SAM enzyme. *Biochemistry 46*, 12889−12895.
(60) Rogge, C. E., Liu, W., Kulmacz, R. J., and Tsai, A. L. (2009) Peroxide-induced radical formation at tyr385 and tyr504 in human PGHS-1. *J. Inorg. Biochem. 103*, 912−922.
(61) Yokoyama, K., Smith, A. A., Corzilius, B., Griffin, R. G., and Stubbe, J. (2011) Equilibration of tyrosyl radicals (Y356$^{\bullet}$, Y731$^{\bullet}$, Y730$^{\bullet}$) in the radical propagation pathway of the *Escherichia coli* class Ia ribonucleotide reductase. *J. Am. Chem. Soc. 133*, 18420−18432.
(62) Frey, P. A., Hegeman, A. D., and Ruzicka, F. J. (2008) The radical SAM superfamily. *Crit. Rev. Biochem. Mol. Biol. 43*, 63−88.
(63) Mccarty, R. M., Krebs, C., and Bandarian, V. (2013) Spectroscopic, steady-state kinetic, and mechanistic characterization of the radical sam enzyme QueE, which catalyzes a complex cyclization reaction in the biosynthesis of 7-deazapurines. *Biochemistry 52*, 188−198.
(64) Booker, S. J. (2012) Radical SAM enzymes and radical enzymology. *Biochim. Biophys. Acta 1824*, 1151−1153.
(65) Krissinel, E., and Henrick, K. (2004) Secondary-structure matching (SSM), a new tool for fast protein structure alignment in three dimensions. *Acta Crystallogr. D60*, 2256−2268.